2011

The role of brookite in mechanical activation of anatase-to-rutile transformation of nanocrystalline TiO2: An XRD and Raman spectroscopy investigation

Masih Rezaee
University of Wollongong

Seyyed Khoie

Hua-Kun Liu
University of Wollongong, hua@uow.edu.au

Recommended Citation

CrystEngComm

PAPER

The role of brookite in mechanical activation of anatase-to-rutile transformation of nanocrystalline TiO$_2$: An XRD and Raman spectroscopy investigation†

Masih Rezaee,[ab] **Seyyed Mohammad Mousavi Khoie**[*a] **and Kun Hua Liu**[b]

The mechanism of phase transformation in nanocrystalline TiO$_2$ powders at ambient temperature during high energy ball milling and the role of brookite phase in anatase-to-rutile phase transformation were investigated by the use of Rietveld analysis of X-ray diffraction patterns and Raman spectroscopy methods. The milling process was performed on a fully anatase phase nanocrystalline TiO$_2$ powder *via* a high energy planetary ball mill with different ball-to-powder weight ratios followed by annealing of the as-milled samples. Some transformation from anatase-to-brookite was observed in all as-milled powders by high resolution transmission electron microscopy. It was proposed that brookite occurs at the {112} twin surfaces of anatase phase and therefore promotes anatase-to-rutile phase transformation. Based on the XRD and Raman results, it was proposed that brookite appears as an essential intermediate phase in mechanically induced anatase-to-rutile phase transformation which facilitates the phase transformation at ambient temperatures and also at higher temperatures during the post-annealing step.

Introduction

Nanocrystalline (nc) titanium dioxide (TiO$_2$) powder has attracted much attention due to its great potential to be used in different applications such as photocatalysis[1] and solar energy conversion.[2] Different parameters are found to be influential on the properties of nc-TiO$_2$ powder and consequently its performance in the mentioned applications.[3–5] Polymorphic phase transformation was reported as one of the most effective parameters in this regard.[4,6] TiO$_2$ has three different polymorphs in ambient conditions including anatase (tetragonal; space group, *I*41/*amd*), brookite (orthorhombic; space group, *Pcab*) and rutile (tetragonal; space group, *P*42/*mnm*) phases.[7] Rutile is the thermodynamic equilibrium phase in ambient pressure neglecting the effect of the grain size.[8]

The grain size of the initial powder is one of most important parameters in determining the phase stability of TiO$_2$, especially in the nanometre scale region.[9] Li *et al.*[10] studied the polymorphic

phase transformation *via* enthalpy calculations and pointed out that the stability of the TiO$_2$ polymorphs is crystallite-size-dependent; anatase is the most stable phase at <11 nm, brookite is the preferable phase at sizes between 11 and 35 nm, while rutile is favored at sizes larger than 35 nm. The grain size of the final product is of interest in different applications. The call for nanocrystalline particles in special applications such as photocatalysis and solar energy conversion,[1,2] has triggered the need to employ low-processing-temperature methods for activating the phase transformation in order to prevent the fast grain growth at high temperatures. As such, mechanical milling, as one of the most convenient processing methods, is widely employed to activate the anatase-to-rutile phase transformation in thermodynamically stable nc-TiO$_2$ powders at ambient temperature.[6,11] Although mechanical activation of such a transformation at ambient temperature seems very interesting, the exact mechanism is still not clear. It is likely that brookite plays an important role in the decrease of the energy barrier required for the mechanical activation of anatase-to-rutile phase transformation at low temperature. Brookite and its role in phase transformation are still ambiguous compared to anatase or rutile, largely due to the difficulties associated with obtaining the brookite phase in the pure form. Furthermore, there is still no agreement among researchers on the reversibility of anatase-to-brookite phase transformation. Although, Zhang and Banfield[10] predicted reversible transformation between anatase and brookite in certain grain size regions, others consider this transformation as an irreversible one.[6]

aMining and Metallurgical Engineering Department, Amirkabir University of Technology, Tehran, Iran. E-mail: m_rezaee@aut.ac.ir; Fax: +0098 (21)64542951; Tel: +0098(21)64542949; mohammad.mousvi@yahoo. com
bInstitute for Superconducting & Electronic Materials (ISEM), ARC Centre for Electromaterials Science, University of Wollongong, Wollongong, Australia. E-mail: hua@uow.edu.au; Fax: +0061(2) 4221 5731; Tel: +0061(2) 4221 4547
† Electronic supplementary information (ESI) available: PXRD data. See DOI: 10.1039/c1ce05185g

Due to the significant effect of phase composition of TiO_2 on the final properties of the milled powders, accurate phase analysis has been attracting much interest among the researchers.[12,13] The ease of data acquisition in the powder diffraction method makes it a vital tool for researchers to get compositional information. The extensive peak broadening due to the presence of nanocrystalline particles results in overlapping of the peaks and makes the phase determination and quantitative analysis process a very demanding and time-consuming procedure. This issue becomes more complicated in mechanically processed powders because of the higher peak overlapping resulting from mechanical strains as the result of induced mechanical impacts, and probably the higher content of impurities resulting from milling jar and balls. Misidentification of multiple phase systems like TiO_2, co-existing in closely related phases, as single phase system can lead to fallacious results. Therefore, full-pattern profile fitting methods of X-ray diffraction patterns such as Rietveld refinement method[14] are extensively employed to assist the phase identification process for the quantification purposes. This powerful method is widely considered to be an intricate and accurate method for microstructural characterization, especially the size–strain analysis of different shapes of nc-TiO_2.[6,12] In spite of the well-known advantages of full-pattern profile fitting methods compared to the conventional methods, there are some delicate points which should be considered during analysis of an X-ray diffraction pattern to achieve reproducible, reliable and accurate results.[15]

As a complementary tool, Raman spectroscopy has already proven to be a reliable method to characterize the small variations in the microstructural characteristics of nc-materials.[16] Raman spectroscopy can provide phase identification and, possibly, size estimation.[16] Correct interpretation of the Raman spectra of nc-TiO_2 powders enables the estimation of various characteristics, such as the existence of mixed phases (anatase in combination with considerable amount of rutile or brookite phase), crystallite size and crystallite size distribution, discrepancy from stoichiometry as well as the type of any stoichiometric defects.[6,12]

This paper addresses a study of the mechanical activation of polymorphic phase transformation in nc-TiO_2 powder by a combination of X-ray diffraction and Raman spectroscopy methods. Rietveld refinement method was employed for full-pattern profile fitting of X-ray diffraction patterns. A mechanism for phase transformation from anatase-to-rutile at ambient temperature at the presence of the brookite phase was proposed.

Experimental procedure

Full anatase phase nanocrystalline TiO_2 powder (Sigma-Aldrich) with mean crystallite size of around 70 nanometres was used as the starting material. Milling was conducted in a high energy planetary ball mill for 3.5 h. A 70 : 30 ratio (weight percent) mixture of 10 millimetres and 5 millimetres in diameter hard chromated steel balls with a ball-to-powder weight ratio of 20 : 1 were used during milling process. Milling was performed at three different speeds of 400, 500 and 600 rpm. As-milled powders were annealed at 850 °C for 2 h to study the effect of post-annealing on the promotion of mechanically activated phase transformation.

Microstructural characterization of both milled and annealed samples was conducted using a GBC MMA X-ray diffractometer (XRD) with Cu-Kα_1 radiation ($\lambda = 1.54056$ Å) in the 2θ range of 20–100° with a step size of 0.02° and a step time of 1.2 s. Quantitative analysis and microstructural parameters determination of the samples were performed via the Rietveld powder structure refinement method employing Materials Analysis Using Diffraction (MAUD) software (Version 2.26).[17] Among available models for strain-size fitting the XRD patterns, Popa fitting model[18] was utilized to cover both isotropic and anisotropic effects. The starting microstructural parameters of the existing phases such as crystal structures, symmetry groups, site occupancies and lattice parameters were taken from the database of the MAUD program. This kind of analysis method takes care of all peaks in the experimental pattern (I_0) (i.e. the observed X-ray powder diffraction pattern of sample) and fits it with respective simulated pattern (I_c). The difference of the calculated value to the experimental one ($I_0 - I_c$) at each point of observation is plotted below each fitted pattern as the goodness of fit (GoF). The lower GoF value plotted at the bottom illustrates the better fitting of the experimental pattern with the simulated one.[17]

The Raman spectroscopy method was also employed to study the phase analysis of the samples and confirm the results calculated based on Rietveld refinement method. Raman spectra were collected by a red laser of 632.8 nanometre wavelength employing a confocal Raman microscope of LabRAM HR, Horiba Jobin Yvon SAS.

Structural changes during mechanical milling process were investigated on a field emission transmission electron microscope (JEOL 3000F FEG TEM).

Results and discussions

Characterization of materials

A graphical representation of XRD patterns of the as-milled samples fitted with their corresponding simulated patterns based on Rietveld refinement method is illustrated in Fig. 1. All the experimental patterns (dots) were fitted with their corresponding simulated pattern (solid lines) employing the Rietveld refinement method. From the difference between the observed and the simulated patterns plotted at the bottom of each pattern, it can be observed that all of them exhibit a proper goodness of fit (GoF). Based on the vertical markers related to different phases at the bottom of Fig. 1, it can be concluded that all as-milled samples exhibit different amounts of the brookite phase. The brookite phase is the most difficult phase to obtain in the phase-pure nanocrystalline form and it is frequently encountered as a by-product of the high pressure processing methods. Brookite is reported to be a high pressure phase.[19] The pressure experienced by anatase powder particles during collision of two colliding balls is estimated to be above 1 GPa and the increase in defect density of anatase due to ball milling may further reduce the lower pressure limit (1.5–10 GPa) required for the transformation of anatase-to-brookite phase.[20] Therefore, the brookite phase, which is a metastable phase at ambient pressure and exists at equilibrium only at high pressures, might be formed during milling conditions.[21] The presence of this phase in
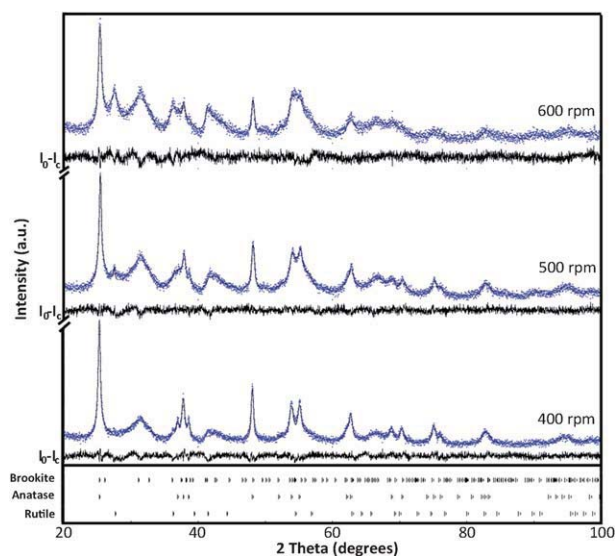
Fig. 1 Graphical representation of XRD patterns of as-milled samples with different milling speeds fitted with their corresponding simulated pattern based on the Rietveld refinement method.

as-milled samples seems to be rational due to the large amount of root mean square (RMS) microstrain imposed on the powders during milling.

According to Fig. 1, it can be observed that all three samples consist of anatase, brookite and rutile phases except the sample milled with 400 rpm which contain no rutile phase. It can also be observed that the peak intensity ascribed to both brookite and rutile phases increase with increasing the milling speed indicating more progression of anatase transformation to these phases. It can be attributed to the higher mechanical activation subjected to the powders upon increasing the milling speed. It is very likely that the faster the mill rotates, the higher would be the energy gained by the powder.[22] The variations of different microstructural parameters of anatase, brookite and rutile TiO_2 phases developed during the milling of the pure anatase TiO_2 powder with different milling speeds are listed in Table 1.

The calculated values for the relative phase content in all three samples (Table 1) are in good agreement with the first estimation of the presence of different phases based on XRD patterns (Fig. 1). As can be seen in this Table, the amount of transformed anatase is increased with increasing milling speed. Increasing the

milling speed from 400 rpm to 500 rpm increases the amount of brookite phase. However, the increase in the milling speed from 500 rpm to 600 rpm results in appearance of the rutile phase in the composition of the as-milled samples. It seems that increasing the milling speed above a critical value, provides enough energy to introduce the required volume contraction to the powder in order to start the brookite-to-rutile phase transformation.[23] The reconstructive anatase-to-rutile phase transformation involves an overall volume contraction of ~8%, while the brookite-to-rutile phase transition is accompanied by a ~3.4% volume contraction.[24] This implies that the brookite-to-rutile phase transformation has a lower barrier energy rather than anatase-to-rutile one.

Raman spectra of three as-milled samples are shown in Fig. 2. Anatase has a body-centered tetragonal structure (space group $I4_1/amd$) containing twelve atoms per unit cell. According to factor group analysis, anatase has six Raman active modes ($A_{1g} + 2B_{1g} + 3E_g$), three infrared active modes ($A_{2u} + 2E_u$) and one vibration of B_{2u} which is inactive in both the infrared and
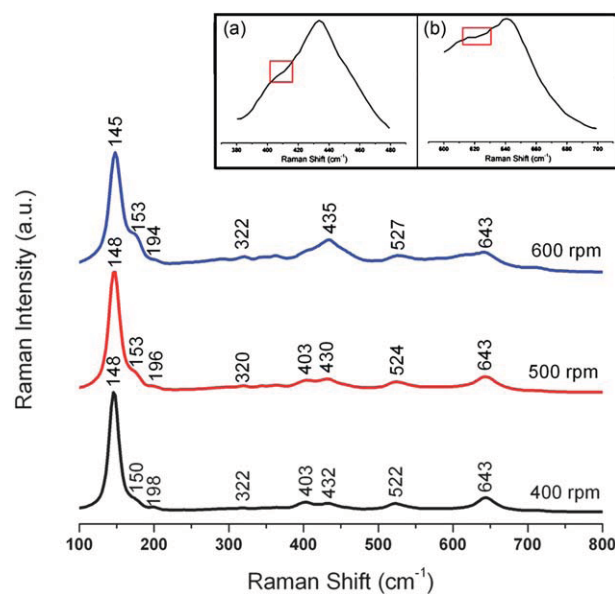

Fig. 2 Raman spectra of three as-milled samples with different milling speeds and magnified Raman bands of the sample milled at 600 rpm (inset) located at (a) ~435 cm^{-1} and (b) ~643 cm^{-1}.

Table 1 Microstructural parameters of as-milled TiO_2 samples calculated by Rietveld refinement method

Milling speed (rpm)	Phases	Lattice parameters/Å			wt (%)	D/nm	RMS microstrain (%)
		a	b	c			
400	Anatase	3.785	3.785	9.519	50.05	70	0.16
	Brookite	9.191	5.475	4.970	49.95	38	1.72
	Rutile	—	—	—	—	—	—
500	Anatase	3.789	3.789	9.531	23.07	54	0.25
	Brookite	9.082	5.530	4.981	75.53	26	1.10
	Rutile	—	—	—	1.40	—	—
600	Anatase	3.777	3.777	9.501	9.46	27	0.31
	Brookite	9.101	5.455	4.942	63.22	64	3.62
	Rutile	4.567	4.567	2.932	27.32	68	0.58

Raman spectra.[25] The Raman bands located at ~144, ~197, ~ 399, ~513, ~519, and ~639 cm^{-1} can be assigned to the anatase phase.[25] There are some blue shifts in all anatase Raman bands of all as-milled samples with changing the milling speed (Fig. 2). Brookite is orthorhombic (*Pbca* space group), has eight formula units per unit cell and shows 36 Raman active modes ($9A_{1g} + 9B_{1g} + 9B_{2g} + 9B_{3g}$). The Raman bands located at about ~150, ~323, ~416, and ~636 cm^{-1} can be ascribed to the brookite phase.[26,27] The most intensive Raman band of brookite is at ~150 cm^{-1} which can influence the width of the E_{1g} Raman mode at ~144 cm^{-1} (ascribed to anatase).[25] The rutile structure has two TiO$_2$ molecules in the unit cell with the space group of *P4$_2$/mnm*. There are six atoms in the unit cell, implying a total of 15 vibration modes. From a group theoretical analysis it can be shown that these 15 modes have the following irreducible representations: $A_{1g} + A_{2g} + A_{2u} + B_{1g} + B_{2g} + 2B_{1u} + E_g + 3E_u$. Further, group theory reveals that four modes, $A_{1g} + B_{1g} + B_{2g} + E_g$ are Raman active and four modes, $A_{2u} + 3E_u$ are infrared active. The other three modes, $A_{2g} + 2B_{1u}$ are neither Raman active nor infrared active.[25] Focusing on some smaller ranges of frequencies (380–480 cm^{-1} (Fig. 2 (inset-a)) and 600–700 cm^{-1} (Fig. 2 (inset-b)) of the Raman spectrum from the sample milled at 600 rpm, a change in the sign of the second derivative of both curves can be observed (inside the squares, inset Fig. 2) which shows there should be two superimposed Raman bands in both cases. The first superimposition might consist of two peaks at ~410 cm^{-1} (assigned to brookite[26,27]) and ~435 cm^{-1} (assigned to rutile[25]). The second superimposition might consist of two peaks at ~613 cm^{-1} (assigned to rutile[25]) and ~643 cm^{-1} (assigned to anatase[26] and/or brookite[26,27]).

The appearance of Raman bands in all samples is in good agreement with the Rietveld calculation of XRD patterns. In particular, the presence of fairly short Raman bands related to rutile phase in the Raman spectrum of the sample milled at 600 rpm before annealing confirms the presence of around 27% rutile in this sample, according to Rietveld refinement calculations.

Graphical representation of XRD patterns of three milled samples after annealing for 2 h at 850 °C is shown in Fig. 3. At the first glance, it can be seen that there is no peak related to the brookite phase. According to the vertical markers at the bottom of the Figure, it can be concluded that all the samples consist of different combinations of anatase and rutile phases. It seems that brookite phase existing in as-milled samples is transformed as a result of annealing at 850 °C. As it was mentioned before, brookite is stable at high pressure[19] and consequently the removal of brookite during annealing can be attributed to the thermal re-crystallization of the microstructure at high temperatures.

The variations of different microstructural parameters of anatase and rutile TiO$_2$ phases developed during annealing of milled samples are listed in Table 2. Quantitative analysis performed by the Rietveld method confirms the conclusions drawn about the relative phase contents of the annealed samples according to the peak shapes. As can be seen in Table 2, the calculated microstrains in all samples are much lower than the values calculated for the as-milled counterparts. It also confirms our conclusion about decreasing the mechanical strains with annealing and its effect on the presence of brookite phase.

Raman spectra of all milled samples after annealing for 2 h at 850 °C are shown in Fig. 4. Comparing these spectra with Fig. 2,
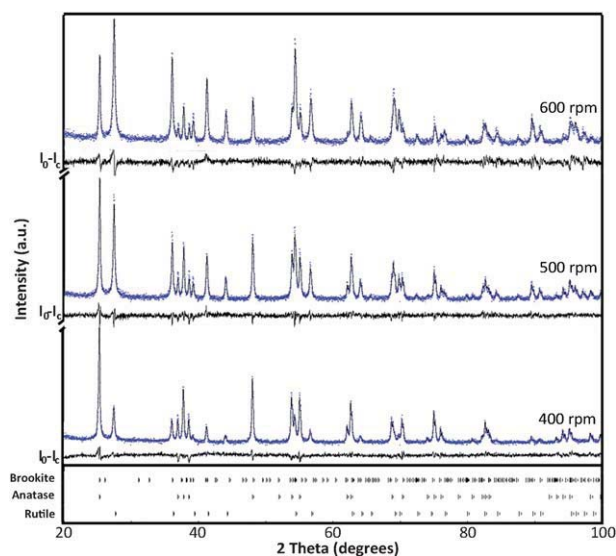

Fig. 3 Graphical representation of XRD patterns of milled samples with different milling speeds after annealing for 2 h at 850 °C, fitted with their corresponding simulated pattern based on the Rietveld refinement method.

it can be concluded that none of the samples includes Raman bands assigned to brookite, which completely confirms the XRD calculations. All the spectra consist of some Raman bands assigned to anatase including the first band (E_g) with highest intensity and some new bands. The Raman bands located at ~235, ~448 and ~612 cm^{-1} can be ascribed to the rutile phase.[25] As can be seen in the Raman spectrum of the sample milled at 400 rpm (Fig. 4), it seems that this sample has no Raman bands related to the rutile phase, which is contrary to the XRD calculations. Focusing on this spectrum in the range of 370–490 cm^{-1} (Fig. 4, inset), a broad band located at ~451 cm^{-1} is observed, which can be assigned to the rutile phase.[25] The other main Raman bands assigned to this phase are not revealed even in the focused spectrum, which suggests that they are hidden in the shoulder of the anatase bands.

Mechanism of mechanically activated phase transformation

In order to have a better understanding of changes in relative phase contents from as-milled samples to the annealed counterparts, these values are plotted as a 3D column curve (Fig. 5).

One interesting point is the variation in anatase content from the as-milled samples to the annealed counterparts. As it can be seen in this curve, the anatase percentage in all as-milled samples is increased by annealing, while the brookite phase was completely removed from all of them. As the rutile percentage is also increased with annealing for all the samples, and also the anatase-to-rutile phase transformation is irreversible,[10] it is proposed that brookite can be transformed back to the anatase phase upon annealing the samples at 850 °C. Penn and Banfield[28] proposed that there is a reversible solid state transformation between the anatase and brookite phases involving displacement of the Ti position. According to the results obtained from the Rietveld refinement method on XRD patterns (Tables 1 and 2), it is proposed that the anatase-to-brookite transition is a reversible

Table 2 Microstructural parameters of milled TiO_2 samples after annealing for 2 h at 850 °C calculated by the Rietveld refinement method

| Milling speed (rpm)	Phases	Lattice parameters/Å		wt (%)	D/nm	RMS microstrain [%]
		a	c			
400	Anatase	3.785	9.520	81.15	277	8.53×10^{-3}
	Rutile	4.593	2.962	18.85	106	0.12
500	Anatase	3.786	9.519	47.25	170	2.22×10^{-2}
	Rutile	4.596	2.960	52.75	112	1.35×10^{-2}
600	Anatase	3.780	9.511	20.29	198	4.62×10^{-2}
	Rutile	4.588	2.959	79.71	126	0.14
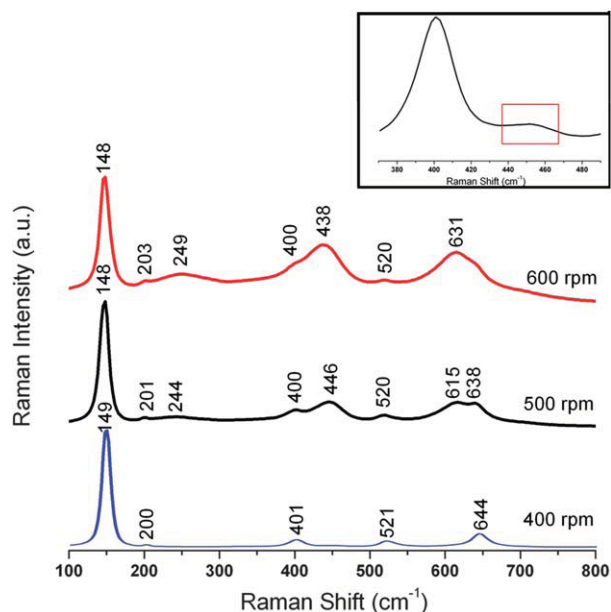
Fig. 4 Raman spectra of three as-milled samples with different milling speeds after annealing for 2 h at 850 °C and magnified Raman band of the sample milled at 400 rpm (inset) located at ~401 cm⁻¹.
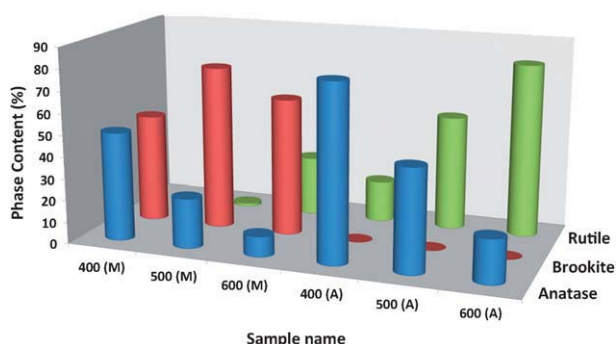
Fig. 5 Relative phase contents (%) calculated from XRD patterns for all milled (M) and annealed (A) samples.

transformation and brookite can act as an intermediate phase to promote the anatase-to-rutile phase transformation. The reverse transformation of brookite to anatase could be a direct result of unstable mechanical strains induced by high-energy ball milling.

According to Fig. 2, a blue shift can be observed in the E_g mode of anatase phase in all as-milled samples with changing the milling speed compared with that reported by Sahoo.[25] There are

two possible reasons for the blue shift of the E_g mode including a phonon confinement effect and the mechanical lattice strain exposed to the powders during the mechanical milling process.[29] Since the crystallite sizes of all samples are larger than ~25 nm, the phonon confinement phenomenon cannot be considered for such a blue shift in the E_g mode. Therefore, the shift in the E_g mode can serve as a direct evidence of mechanical lattice strain in anatase crystals. In a tetragonal system like anatase, the E_g mode is much more sensitive to an out-of-phase motion of oxygen atoms along the c-axis than the Ti–O stretching mode.[30] Since the milling process was conducted in air atmosphere, oxygen depletion is a less likely parameter to affect the motion style of oxygen atoms. On the contrary, the change in crystal positions of oxygen atoms in anatase phase can be considered as a much more influential phenomenon which can be considered as the main parameter affecting the blue shift of E_g mode in Raman spectra of as-milled samples, consequently leading to high amounts of mechanical strain. According to the results of Rietveld refinement calculations on the as-milled samples (Table 1), the RMS microstrain in all of the samples is more than ~0.15%. Introduction of the mechanical distortion to the crystal lattice of the powders is a definite result of the milling process.

Bégin-Colin *et al.*[21] proposed a general mechanism for mechanically induced phase transformation from anatase-to-rutile as "anatase → brookite → rutile" whatever the milling conditions. Thermodynamic stability of the initial anatase powder used in this work was thoroughly studied during annealing and no phase transformation was observed based on the XRD pattern (Fig. 6), even after annealing for 20 h at 850 °C. The milling process is known to generate defect accumulation and particle size reduction. The local temperature on the surface of the powders increases during the milling which contributes to
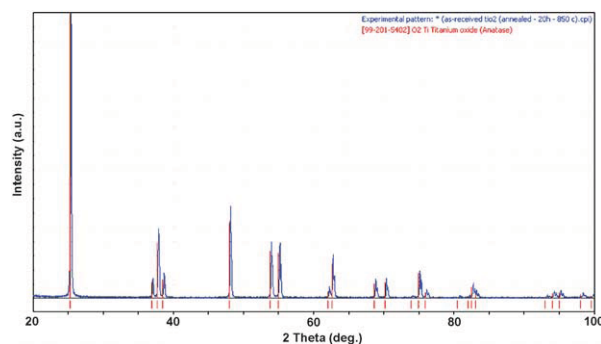
Fig. 6 XRD pattern of as-received anatase annealed for 20 h at 850 °C.

the activation of solid compounds so that they store additional energy which facilitates chemical reactions or transformations.[21] According to the relative phase content in the as-milled samples (Table 1), mechanical activation of phase transformation at ambient temperature is a valid argument. According to Table 1, it is proposed that brookite is an essential part of the mechanically activated phase transformation in TiO_2. Penn and Banfield[28] proposed that brookite occurs at some {112} twin surfaces, according to the high resolution transmission electron microscopy results. Because {112} anatase twin interfaces contain one unit cell of brookite, they suggested that brookite may nucleate at twin planes and grow at the expense of anatase; therefore, the transformation of anatase-to-brookite is much easier than its transformation to rutile. High resolution transmission electron microscopy (HRTEM) results support the assertion that brookite occurs at some {112} twin surfaces of the anatase phase. Fig. 7 shows an HRTEM micrograph of the sample milled at 600 rpm. The distance between both series of lattice fringes marked in this Figure was measured to be 0.23 nm corresponding to d-spacing of {112} crystal planes in anatase phase (00-001-562 PDF file). As illustrated in Fig. 7, a brookite cell nucleates on the twinning interface of these two {112} crystal planes of anatase phase. When a crystal deforms plastically by twinning, atomic displacements occur at distances lower than an inter-atomic separation. The twinning phenomenon needs to be activated thermally or mechanically. Both high strain rates and low temperatures are known to promote twinning.[28] As the milling process is performed at ambient temperature and produces high strain rates,[20] mechanical strain is proposed to activate this phenomenon.

Penn and Banfield[28] inferred that the anatase-to-rutile phase transformation in nanocrystalline materials is rate limited by rutile nucleation, as opposed to rutile growth. They proposed that oriented attachment of primary particles between brookite and anatase {112} crystallites and their growth can lead to the formation of planar defects, including twin planes and other interfaces.[28] They proposed that such interfaces with a rutile-like character should result in decreased activation barriers for rutile nucleation and thus, contribute significantly to the observed faster transformation rates in nanocrystalline materials compared to coarse crystalline counterparts.[28] By comparing the brookite content of the as-milled samples and calculating the difference in rutile content between as-milled and annealed samples (Tables 1 and 2) (18.85%, 51.35% and 52.39% for
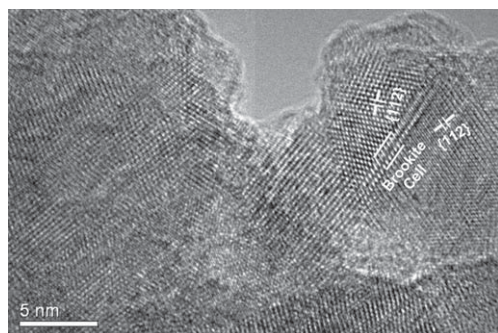

Fig. 7 HRTEM micrograph of the sample milled at 600 rpm before annealing.

different milling speeds of 400, 500 and 600 rpm), it can be concluded that the presence of brookite phase in the primary particles can promote the anatase-to-rutile phase transformation.[19] As it was mentioned before, the energy barrier of anatase-to-brookite and brookite-to-rutile phase transformations are lower than that of anatase-to-rutile phase transformation.[28] As mechanical milling is performed at ambient temperature, the presence of brookite as an intermediate high pressure phase is proposed to be necessary in mechanically activated anatase-to-rutile phase transformations to facilitate the anatase-to-rutile phase transformation.

Conclusions

Mechanical activation of anatase-to-rutile phase transformation in nanocrystalline TiO_2 phase was studied by the use of XRD and Raman spectroscopy methods. Based on the calculations conducted on XRD patterns *via* Rietveld refinement method, it was found that increasing the milling speed can lead to increasing the mechanical energy imposed to the powders and then promoting the phase transformation from anatase to brookite and rutile phase. According to the blue shift of E_g Raman mode of all as-milled samples and the calculated microstrain from XRD patterns, the appearance of brookite as an intermediate phase was proposed as a mechanism for a mechanically induced transformation which can facilitate the anatase-to-rutile phase transformation of a thermally stable powder at ambient temperature.

Acknowledgements

Notes and references

1 A. Di Paola, G. Cufalo, M. Addamo, M. Bellardita, R. Campostrini, M. Ischia, R. Ceccato and L. Palmisano, *Colloids Surf., A*, 2008, **317**, 366–376.
2 K. Cheng-Yu and L. Shih-Yuan, *Nanotechnology*, 2008, **19**, 095705.
3 E. Arca, G. Mulas, F. Delogu, J. Rodriguez-Ruiz and S. Palmas, *J. Alloys Compd.*, 2009, **477**, 583–587.
4 P. Billik, G. Plesch, V. Brezová, L. Kuchta, M. Valko and M. Mazúr, *J. Phys. Chem. Solids*, 2007, **68**, 1112–1116.
5 A. Dodd, A. McKinley, T. Tsuzuki and M. Saunders, *J. Phys. Chem. Solids*, 2007, **68**, 2341–2348.
6 M. Rezaee and S. M. Mousavi Khoie, *J. Alloys Compd.*, 2010, **507**, 484–488.
7 J. Zhu, J.-X. Yu, W. Y-J., C. X-R. and J. F-Q., *Chin. Phys. B*, 2008, **17**, 2216.
8 M. Salari, S. M. Mousavi khoie, P. Marashi and M. Rezaee, *J. Alloys Compd.*, 2009, **469**, 386–390.
9 D. J. Reidy, J. D. Holmes and M. A. Morris, *J. Eur. Ceram. Soc.*, 2006, **26**, 1527–1534.
10 S. Li, Z. H. Jiang and Q. Jiang, *Mater. Res. Bull.*, 2008, **43**, 3149–3154.
11 F. Delogu, *J. Alloys Compd.*, 2009, **468**, 22–27.
12 S. Murugesan, P. Kuppusami and E. Mohandas, *Mater. Res. Bull.*, 2010, **45**, 6–9.

13 K. Sakurai and M. Mizusawa, *Anal. Chem.*, 2010, **82**, 3519–3522.
14 R. Carrera, N. Castillo, E. Arce, A. L. Vázquez, M. Moran-Pineda, J. A. Montoya, P. Del Ángel and S. Castillo, *Res. Lett. Nanotechnol.*, 2008, **2008**, 1–5.
15 M. R. Panigrahi and S. Panigrahi, *Phys. B*, 2010, **405**, 3986–3990.
16 G. Gouadec and P. Colomban, *J. Raman Spectrosc.*, 2007, **38**, 598–603.
17 L. Lutterotti, MAUD – Materials Analysis Using Diffraction (New version: 2.26), http://www.ing.unitn.it/~maud/.
18 N. C. Popa and D. Balzar, *J. Appl. Crystallogr.*, 2008, **41**, 615–627.
19 J.-G. Li, T. Ishigaki and X. Sun, *J. Phys. Chem. C*, 2007, **111**, 4969–4976.
20 P. Bose, S. K. Pradhan and S. Sen, *Mater. Chem. Phys.*, 2003, **80**, 73–81.
21 S. Bégin-Colin, T. Girot, G. Le Caër and A. Mocellin, *J. Solid State Chem.*, 2000, **149**, 41–48.

22 C. Suryanarayana, *Prog. Mater. Sci.*, 2001, **46**, 1–184.
23 K. Gheisari, S. Javadpour, J. T. Oh and M. Ghaffari, *J. Alloys Compd.*, 2009, **472**, 416–420.
24 D. Hanaor and C. Sorrell, *Mater. Sci.*, 2010, **46**, 1–20.
25 S. Sahoo, A. K. Arora and V. Sridharan, *J. Phys. Chem. C*, 2009, **113**, 16927–16933.
26 A. Golubović, M. Šćepanović, A. Kremenović, S. Aškrabić, V. Berec, Z. Dohčević-Mitrović and Z. Popović, *J. Sol-Gel Sci. Technol.*, 2008, **49**, 311–319.
27 Y. Shu, K. Ihara, B. Liu, Y. Wang, R. Li and T. Sato, *Phys. Scr.*, 2007, **2007**, 268.
28 R. L. Penn and J. F. Banfield, *Am. Mineral.*, 1999, **84**, 871–876.
29 V. Swamy, *Phys. Rev. B: Condens. Matter Mater. Phys.*, 2008, **77**, 195414.
30 J. Wang, Q. Zhang, S. Yin, T. Sato and F. Saito, *J. Phys. Chem. Solids*, 2007, **68**, 189–192.